Article:

Whiteside, E.A., Fairclough, H.E. and Rigby, S.E. (2026) Fail-safe optimization concerning partial damage—a comparison of rigid plastic and linear elastic material models. Structural and Multidisciplinary Optimization, 69 (6). 163. ISSN: 1615-147X

https://doi.org/10.1007/s00158-026-04360-4

Structural and Multidisciplinary Optimization (2026) 69:163
https://doi.org/10.1007/s00158-026-04360-4

BRIEF NOTE

Fail-safe optimization concerning partial damage—a comparison of rigid plastic and linear elastic material models

Edward A. Whiteside[1] · Helen E. Fairclough[1] · Sam E. Rigby[1]

Received: 27 January 2026 / Revised: 17 April 2026 / Accepted: 15 May 2026 / Published online: 13 June 2026

Abstract
Existing studies on stress-constrained fail-safe optimization concerning partial damage with elastic material models have shown that the partial degradation of a member may cause a worse objective function than complete removal. This brief note compares the results of a simple formulation using a rigid plastic material with those of the existing elastic problem, using a three-bar example as an illustration. It is demonstrated that the plastic formulation resolves the singularity issues, and the underlying characteristics of both formulations can be understood from both a mathematical and an intuitive engineering perspective. As well as remaining continuous at complete damage, plastic load redistribution enables optimum volumes to be 80% lower than the elastic optimum in cases approaching complete damage. Investigations into the workings of the problems unveil their inherent strengths and weaknesses, and thus areas for future improvement.

Keywords Fail-safe optimization · Partial damage · Disproportionate collapse · Size optimization

1 Introduction

In a short study concerning the stress-constrained fail-safe optimization of elastic structures subject to partial damage, Dou and Stolpe (2021) revealed unique singularity characteristics. By considering a three-bar cantilever problem with damage modelled as a partial reduction of the cross-sectional area, it was demonstrated that the transition from near-complete to complete element removal reveals a singularity of the optimum objective function, with the near-complete damage possessing a significantly larger solution value. Similar results were found in a subsequent study by Dou and Stolpe (2022) on fail-safe optimization of beam structures subject to stress and eigenfrequency constraints. Such a phenomenon bears similarity to the design-space singularity issue discussed in Kirsch (1990), Cheng and Jiang (1992), Rozvany (2001), as the transition from partial to complete damage modifies the elastic compatibility functions, removing constraints from the problem and thereby causing jumps in the problem's optimum.

Dou and Stolpe (2021) employed an elastic formulation, where the system's stiffness determines the attainment of equilibrium. For traditional stress-constrained problems with design-space singularity issues, relaxing the elastic compatibility along with the introduction of explicit state variables removes these issues (Kirsch 1990). This relaxation and additional variables, in conjunction with local element stress constraints, lead the structural response to adhere to a rigid-plastic material model. While, in general, this relaxation does not lead to a significant difference in optimal solutions (e.g. Weldeyesus et al. 2019), this study shows that, for partial-damage fail-safe optimization, the singularity problems are removed and the optima for intermediate damage levels are substantially different.

2 Rigid plastic formulation

Here, a simple adaptation to Fairclough et al. (2023)'s linear rigid plastic fail-safe optimization formulation is presented. Damage is modelled as described in Dou and Stolpe (2021), where each damage case refers to the partial reduction of an element's cross-sectional area, governed by the constant γ.

Responsible Editor: Tomas Zegard.

✉ Helen E. Fairclough
helen.fairclough@sheffield.ac.uk

[1] School of Mechanical, Aerospace, and Civil Engineering, The University of Sheffield, Sir Fredrick Mappin Building, Mappin St., S1 3JD Sheffield, UK

The fail-safe problem $P_{FS}|_{\gamma=[0,1]}$ can be written as

$$\min_{\mathbf{a},\,\mathbf{q}_k\,\forall k} \quad \mathbf{L}^T\mathbf{a} \tag{1a}$$

$$\text{s.t.} \quad \mathbf{B}\mathbf{q}_k + \mathbf{f} = \mathbf{0} \qquad \forall k \tag{1b}$$

$$\mathbf{q}_k - \sigma_y \mathbf{D}_k \mathbf{a} \leq \mathbf{0} \qquad \forall k \tag{1c}$$

$$-\mathbf{q}_k - \sigma_y \mathbf{D}_k \mathbf{a} \leq \mathbf{0} \qquad \forall k \tag{1d}$$

$$\mathbf{a} \geq \mathbf{0} \tag{1e}$$

where $\mathbf{a}$ and $\mathbf{q}_k$ are vectors of explicit optimization variables, representing cross-sectional areas, and internal axial forces for a damage case k, respectively. $\mathbf{L}$ is a vector of element lengths within the structure and σ_y is the material yield stress. $\mathbf{B}$ is an equilibrium matrix for resolving internal element forces, and $\mathbf{f}$ is the external load vector. Finally, $\mathbf{D}_k$ is the partial damage matrix for a given damage case k. This matrix is a diagonal matrix comprised of 1 s, with $(1-\gamma_{i,k})$ placed in the row and column corresponding to the damaged elements, and thus formally defined as

$$\mathbf{D}_k = \mathbf{I} - \sum_{i \in \mathbb{K}_k} \gamma_{i,k} \mathbf{e}_i \mathbf{e}_i^T \tag{2}$$

where $\mathbf{I}$ is the identity matrix, and $\mathbf{e}_i$ is the standard basis vector, with the 1 placed at the index i. $\mathbb{K}_k$ defines the damaged elements for damage case k.

In this study, the same damage factor is applied to all damaged elements, and such factors are assumed to be of the same magnitude for all damage cases, giving a single value γ for a given problem.

The nominal non-fail-safe problem (P_N) can be given by making $\gamma = 0$ (e.g. $P^*_{FS}|_{\gamma=0} = P^*_N$). Consequently, the feasible set of the fail-safe problem can thus be thought of as an equal or subset of the nominal problem feasible set ($\mathbb{F}_{FS} \subseteq \mathbb{F}_N \;\; \forall k$), meaning that, provided that all P_{FS} have solutions, $P^*_{FS}|_{\gamma=(0,1]} \geq P^*_N$.

3 Three-bar cantilever example

Here, the same three-bar structure example as used in Dou and Stolpe (2021) is considered for direct comparison. The structure, damage cases, and optimization variables for the plastic formulation are given in Fig. 1. The following properties are applied: $f = 1$ $\sigma_y = 1$; $L = 1$

In the form using (1), the problem consists of 12 variables (Fig. 1) and 27 constraints. However, complexity can be reduced while maintaining accuracy by exploiting the problem's symmetry and other inherent properties to eliminate redundant damage cases, variables, and constraints. The steps for reducing the problem are fully detailed in the supplementary material. The problem is reduced such that the outer bars are linked to a single design variable, a_1, and only the first damage case is considered, with stress constraints for the correct internal force directions for the applied load and damage case. Hence, the reduced problem now consists of five variables with seven constraints, and can be written as

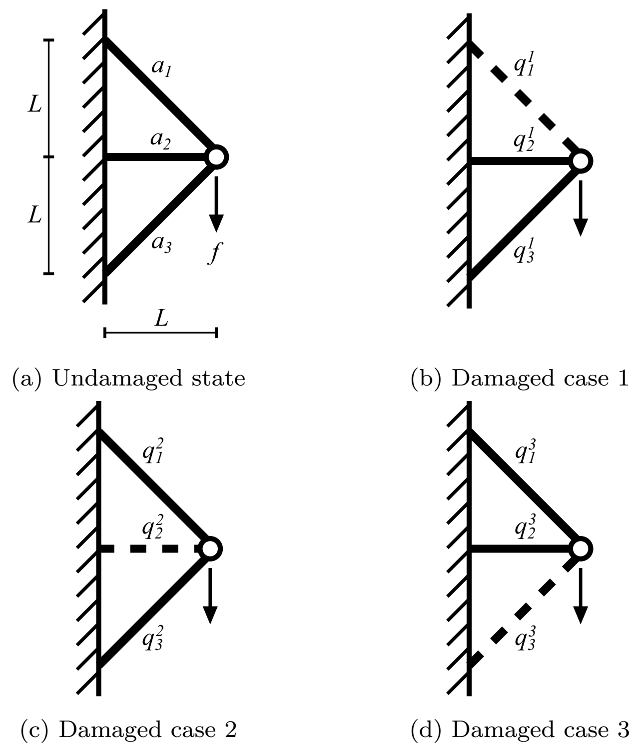

Fig. 1 Three-bar example structure subject to single element damage. Dashed lines denote damaged elements. **a** Undamaged structure and design variables. **b–d** Damage cases and internal force variables

$$\min_{\mathbf{a},\,\mathbf{q}} \quad 2\sqrt{2}a_1 + a_2 \tag{3a}$$

$$\text{s.t.} \quad \begin{bmatrix} -\frac{\sqrt{2}}{2} & -1 & -\frac{\sqrt{2}}{2} \\ \frac{\sqrt{2}}{2} & 0 & -\frac{\sqrt{2}}{2} \end{bmatrix} \begin{bmatrix} q_1 \\ q_2 \\ q_3 \end{bmatrix} + \begin{bmatrix} 0 \\ -1 \end{bmatrix} = \begin{bmatrix} 0 \\ 0 \end{bmatrix} \tag{3b}$$

$$\begin{bmatrix} q_1 \\ q_2 \\ -q_3 \end{bmatrix} - \sigma_y \begin{bmatrix} (1-\gamma) & 0 & 0 \\ 0 & 1 & 0 \\ 0 & 0 & 1 \end{bmatrix} \begin{bmatrix} a_1 \\ a_2 \\ a_1 \end{bmatrix} \leq \begin{bmatrix} 0 \\ 0 \\ 0 \end{bmatrix} \tag{3c}$$

$$a_1, a_2 \geq 0. \tag{3d}$$

To investigate the elastic formulation's properties, Dou and Stolpe (2021) conducted a parametric study on γ. The same is performed here. The reduced problem (3) is considered to aid visualization and investigation; however, the parametric study was also performed using the complete formulation (1), and the optimal values were found to be identical.

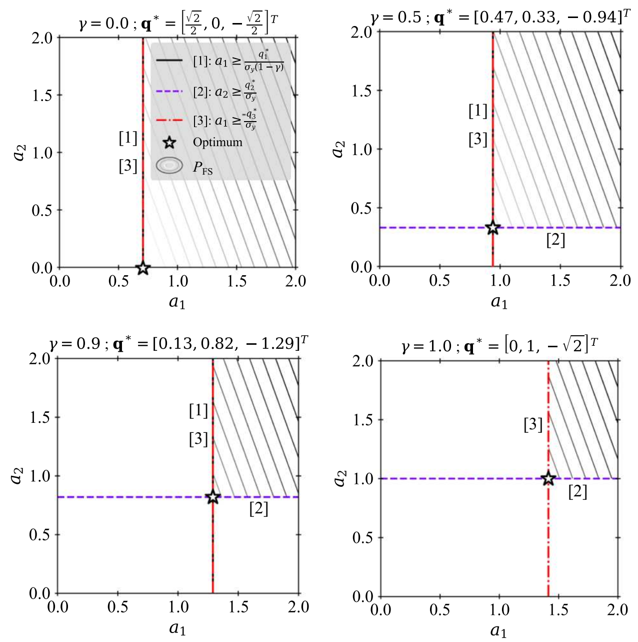

Fig. 2 Reduced design spaces of variables a_1 and a_2 considering a constant feasible internal force vector, taken as $\mathbf{q}^*$, for varying levels of damage, $\gamma = \{0, 0.5, 0.9, 1\}$

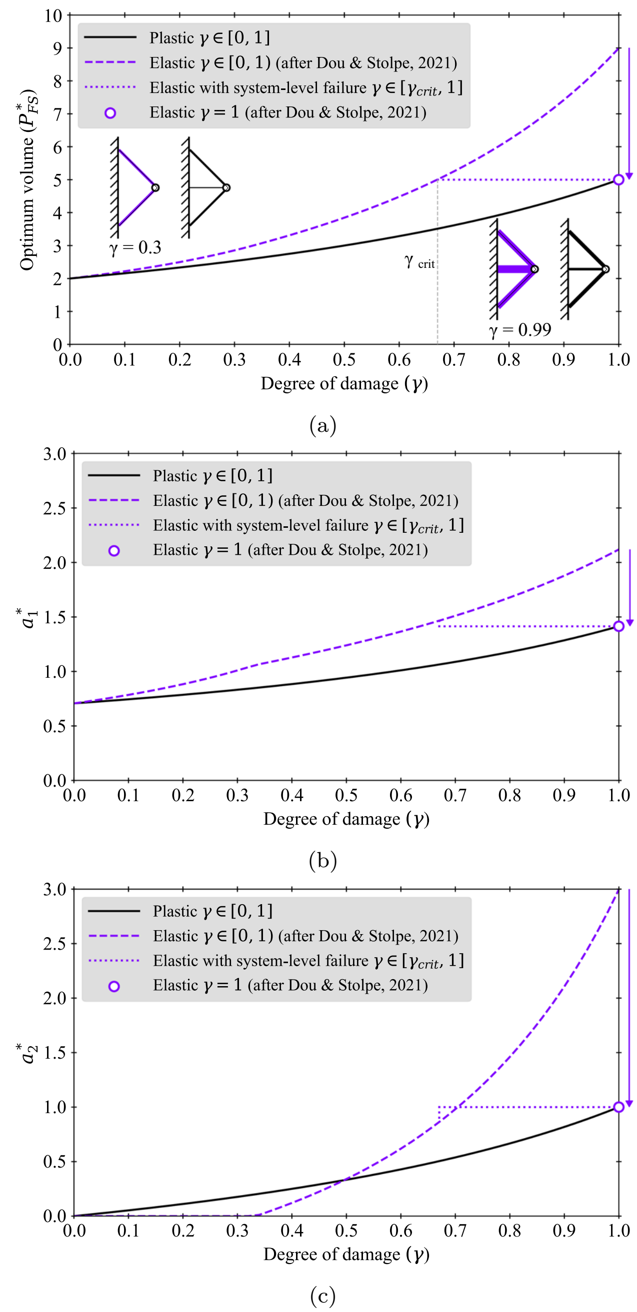

Fig. 3 Optimum volumes and areas for varying degrees of damage, comparing results from the presented plastic formulation, Dou and Stolpe (2021)'s elastic formulation, and expected results from an elastic formulation with a system-level failure definition. $\gamma_{crit} \approx 0.67$. **a** Optimum volumes (P^*_{FS}) and illustrations of resulting structures. **b** Optimum areas of inclined elements (a_1^*). **c** Optimum areas of horizontal element (a_2^*)

The problem is composed of five explicit optimization variables, meaning the total variable space cannot be visualized. However, by considering that (3b) will produce a set of feasible values of internal forces, and selecting a point within that feasible set, one can consider a reduced design space of the variables a_1 and a_2 and the binding of the yield constraints (3c) with the condition of the constant internal forces. Here, the optimum internal forces, $\mathbf{q}^*$, are chosen to visualize the problems, and are presented in Fig. 2.

While Fig. 2 does not encompass the entire feasible design space, it offers an intuitive interpretation of the problem for varying levels of element damage. One can see that the increased level of damage corresponds to a reduction of the reduced design space, with no sudden changes observed during the transition from partial to complete damage. A mathematical proof that his behaviour will always hold can be found in the supplementary material. Likewise, the position of the optimum exhibits a smooth shift. The optimum solutions for a continuous change in damage compared to those derived from Dou and Stolpe (2021)'s elastic formulation are illustrated in Fig. 3.

The elastic and plastic results at the extremities of damage ($\gamma = 0, 1$) are identical. For low damage levels, the elastic and plastic optimum volumes remain similar; however, they diverge rapidly. Whilst the elastic formulation makes no use of the horizontal element until a critical level of damage occurs, the plastic formulation makes use of all elements for any non-zero values of damage. Furthermore, when transitioning from high cross-section degradation to complete removal, as indicated by the change in feasible region shown in Fig. 2, no singularity is observed for the plastic formulation.

The subsequent sections explore the explanation for the deviation in results, considering both the mathematical nature of the problems and the engineering characteristics they model.

4 A mathematical interpretation

The rationalization given by Dou and Stolpe (2021) for the singularity effect of the elastic problem is that as $\gamma < 1$ goes to $\gamma = 1$, an active constraint switch occurs. For $\gamma < 1$, the optimum is governed by a single stress constraint corresponding to the damaged element; however, when $\gamma = 1$, the element is effectively removed from the structure, thus removing the constraint from the system. This results in a sudden shift in the feasible set, thereby inducing a significant change to the problem solution.

For the plastic formulation, multiple stress constraints are active. This is a consequence of the polyhedral feasible space, with the position of an optimum always occurring at a vertex of this space. For the three-bar example problem, when $\gamma < 1$, due to the existence of the two equality constraints, at least three constraints must be active to form a solution. When $\gamma = 1$, the formulation, like the elastic problem, will effectively remove the damaged element yield constraints from the problem. Concerning $\gamma < 1$, provided that $P^*_{FS} > P^*_N$, a damaged element yield constraint must be active. Although the transition to $\gamma = 1$ will remove this constraint, the dimensions of the variable space will also have decreased, meaning one less constraint is required to form the optimum vertex. The active undamaged element constraints for $\gamma < 1$ will maintain the vertex of this new space. This can be observed in the reduced feasible space in Fig. 2 for the three-bar problem, where all three stress constraints are active for partial damage scenarios. The damaged constraint $a_1 \geq \frac{q_1^*}{\sigma_y(1-\gamma)}$ is removed, but the remaining elements still bound the problem. Note that this behaviour is inherent to the linear program and will occur for any problem size where multiple damage cases may inform the optimum.

An alternative perspective is that an increase in γ will result in a relaxation of the yield constraint, thereby resulting in the feasible sets being decreased, and consequently, $P^*|_{\gamma=g} \leq P^*|_{\gamma=h}$ where $g \leq h$. Hence, any increase in γ cannot result in a decrease in the optimum objective function, meaning the singularity jump observed in the elastic formulation cannot occur in the proposed plastic. A full proof of this corollary is given in the supplementary material.

When $\gamma = 1$ for the three-bar example, the solutions from the plastic and elastic formulations are identical; this can be easily rationalized by the fact that both structures in their damaged states are statically determinate, meaning the force distribution is constant, irrespective of design variables a. Consequently, the stress constraints for both formulations input the same forces, and thus, are mathematically identical. However, in general, when the damaged ground structure is indeterminate, solutions may deviate.

5 An engineering interpretation

5.1 Elastic formulation

Dou and Stolpe (2021) provides an explanation of the singularity phenomenon by demonstrating how, for a fixed area structure, an increase in degradation will increase the structure's maximum stress until complete removal. Equally, this behaviour can be understood from a strain perspective, where, as a consequence of the equilibrium conditions that implement elastic compatibility, the stress constraints also impose a strain limit on each element. This implies a brittle material model, thereby prohibiting any form of load redistribution through plasticity. The material model thus leads to an element-level definition of structural failure. That is, if any element exceeds this strain limit, the entire structure is deemed to have failed. This limits the structure's capacity to the strain of the damaged element, thereby increasing element volumes at high damage levels.

As illustrated by the results of Dou and Stolpe (2021), for certain levels of partial damage, a more optimal solution could be found if the constraints allowed for breakage of the degraded element post-damage. This highlights the benefits of reevaluating how one defines disproportionate collapse in elastic fail-safe optimization, and that a more system-level failure definition may be beneficial where the state of the entire structure defines when it fails. Such problems may come in many forms, for example, a definition which considers the collapse of the total structure, such as the approach taken by da Silva et al. (2023, 2024) in reliability-based optimization, or perhaps failure defined through excessive deflection.

For simple problems, it is possible to relax the elastic problem by checking each combination of 'snapped' ($\gamma = 1$) and un-snapped ($\gamma < 1$) constraints for all damage cases; giving the results in Fig. 3. for an exact formulation. However, this approach (with 2^K possible combinations to check) will become rapidly impractical for larger problems, and so future work is suggested to investigate how concepts from reliability-based optimization and/or discrete optimization may be employed here.

5.2 Plastic formulation

Whilst the elastic formulation limits element strain, the presented plastic formulation utilizes a rigid plastic model, resulting in an infinite permissible strain, and thus significant implications for the structural response and its handling of partial damage.

The immediate consequence is that internal load redistribution through plasticity may occur. Thus, when an element yields, unyielded elements can resist the additional forces, and therefore, the strength of the structure is not limited by the capacity of the damaged component. The other consequence of the infinite strain capacity is that an element cannot break under loading, and thus, local progressive failure cannot occur. The structure will instead redistribute the loads until force equilibrium cannot be maintained (following the lower-bound theory of plastic limit analysis (Moy 1981)). At the limit of capacity, the structure becomes a mechanism, and thereby fails in a global state, a characteristic illustrated by the kinematic dual formulation of problem P, which optimizes the virtual displacement fields to determine these mechanism states (see supplementary material for details). Thus, failure is not defined at the local level but at a system level.

Due to the structure's ability to redistribute loads and not use a local element failure definition, the optimizer does not need to 'protect' the damaged element, and instead can make greater use of the undamaged structure. Due to this additional strength, the optimum structures produced by the plastic formulation will be equally, or even more, materially efficient than those produced by the elastic formulation.

6 Conclusions and recommendations

This work is a response to Dou and Stolpe (2021)'s study on elastic stress-constrained fail-safe optimization problems for sizing truss structures subject to partial structural damage. The use of a simple linear programming formulation incorporating a plastic material has been demonstrated to resolve the issue of objective function singularity when transitioning from partial to complete element damage. Plastic results were also shown to be more or equally materially efficient than the elastic results for all damage levels.

The underlying behaviour of the two formulations can be understood through the mathematical nature of the problems or, from an intuitive engineering perspective by considering the material model characteristics. The difference in results is due to the elastic formulation's reliance on a single-element definition of structural failure, whereas the plastic problem uses a more global definition. The elastic formulation's failure definition is overly conservative, and efficiency gains can be made by incorporating a more system-level definition. Formulations that employ selection of constraint-sets (i.e. partial damage or complete damage) may be an alternative to achieve a similar outcome.

Author Contributions Edward A. Whiteside: Conceptualization, Methodology, Formal analysis and investigation, Writing—original draft preparation, and Writing–review and editing; Helen E. Fairclough: Conceptualization, Methodology, Writing—review and editing, and Supervision; and Sam E. Rigby: Conceptualization, Methodology, Writing—review and editing, and Supervision

Funding This work was supported by a Faculty of Engineering Studentship from the University of Sheffield.

Declarations

Conflict of interest The authors declare that they have no known competing financial interests or personal relationships that could have appeared to influence the work reported in this paper.

Replication of results: Required equations are given in the text and can be solved using any available convex or linear solvers.

References

Cheng G, Jiang Z (1992) Study on topology optimization with stress constraints. Eng Optim 20(2):129–148. https://doi.org/10.1080/03052159208941276

da Silva LAR, Torii AJ, Beck AT (2023) Hyperstatic and redundancy thresholds in truss topology optimization considering progressive collapse due to aleatory and epistemic uncertainties. Probab Eng Mech 71:103384. https://doi.org/10.1016/j.probengmech.2022.103384

da Silva LAR, Torii AJ, Beck AT (2024) System-reliability-based sizing and shape optimization of trusses considering millions of failure sequences. Struct Saf 108:102448. https://doi.org/10.1016/j.strusafe.2024.102448

Dou S, Stolpe M (2021) On stress-constrained fail-safe structural optimization considering partial damage. Struct Multidisc Optim 63(2):929–933. https://doi.org/10.1007/s00158-020-02782-2

Dou S, Stolpe M (2022) Fail-safe optimization of tubular frame structures under stress and eigenfrequency requirements. Comput Struct 258:106684. https://doi.org/10.1016/j.compstruc.2021.106684

Fairclough HE, He L, Asfaha TB, Rigby S (2023) Adaptive topology optimization of fail-safe truss structures. Struct Multidisc Optim 66(7):148. https://doi.org/10.1007/s00158-023-03585-x

Kirsch U (1990) On singular topologies in optimum structural design. Struct Optim 2:133–142. https://doi.org/10.1007/BF01836562

Moy SS (1981) Plastic methods for steel and concrete structures. Springer

Rozvany G (2001) On design-dependent constraints and singular topologies. Struct Multidisc Optim 21:164–172. https://doi.org/10.1007/s001580050181

Weldeyesus AG, Gondzio J, He L, Gilbert M, Shepherd P, Tyas A (2019) Adaptive solution of truss layout optimization problems with global stability constraints. Struct Multidisc Optim 60:2093–2111. https://doi.org/10.1007/s00158-019-02312-9